Porous Ni Electrodes Modified with Au Nanoparticles for Hydrogen Production

V. Pérez-Herranz, C. González-Buch, E. M. Ortega, S. Mestre

Abstract**—**In this work new macroporous Ni electrodes modified with Au nanoparticles for hydrogen production have been developed. The supporting macroporous Ni electrodes have been obtained by means of the electrodeposition at high current densities. Then, the Au nanoparticles were synthesized and added to the electrode surface. The electrocatalytic behaviour of the developed electrocatalysts was studied by means of pseudo-steady-state polarization curves, electrochemical impedance spectroscopy (EIS) and hydrogen discharge curves. The size of the Au synthetized nanoparticles shows a monomodal distribution, with a very sharp band between 10 and 50 nm. The characteristic parameters d10, d50 and d90 were 14, 20 and 31 nm respectively. From Tafel polarization data has been concluded that the Au nanoparticles improve the catalytic activity of the developed electrodes towards the HER respect to the macroporous Ni electrodes. EIS permits to obtain the electrochemically active area by means of the roughness factor value. All the developed electrodes show roughness factor values in the same order of magnitude. From the activation energy results it can be concluded that the Au nanoparticles improve the intrinsic catalytic activity of the macroporous Ni electrodes.

Keywords**—**Au nanoparticles, hydrogen evolution reaction, porous Ni electrodes.

I. Introduction

HYDROGEN is considered an ideal energy carrier that can be an alternative to fossil fuels. It is a clean and fully recyclable substance with a practically unlimited supply and has all the criteria considered for an alternative energy source [1], [2]. The electrochemical production of hydrogen by alkaline water electrolysis is one of the most promising methods with great potential of using renewable energy sources, such as solar energy [3], [4]. Also it represents an environmentally friendly technology for production of high purity hydrogen [1]. However, the high-energy consumption of alkaline water electrolysis retrains its large-scale application at present. In order to make this technique more efficient and economical, both the decrease of the over-potentials of electrode reactions and the selection of inexpensive electrode materials with good electro-catalytic activity are needed.

Noble metals such as platinum and ruthenium are the most active materials towards the HER but both their cost and scarcity restrain their use as cathode material for the large-scale alkaline water electrolysis. For this reason, there are a lot of researches for replacing the Pt by low cost and active catalytic materials. Most of these materials are Ni-based alloys: NiCo [5], [6], NiFe [7], [8], NiMo [9], [10], NiW [11], [12], NiCu [13], NiAl [14], [15], NiZn [16]; because Ni is a good catalyst and it has high corrosion resistance in alkaline media.

In the last years, the development of nanoparticle catalysts has had a great interest because it not only allows using a small amount of material, but also provides a larger active surface area [17]. The metal nanoparticles need to be synthesized first and then assembled on the electrode [18]. The use of a macroporous electrode as a supporting material can reduce the dosage of noble metals [19].

The aim of the present work is the enhancement of the catalytic activity for the HER in macroporous Ni by incorporating Au nanoparticles on the electrode surface. The presence of the Au nanoparticles has been confirmed by means of FE-SEM microscopy and the EDX analysis. The electrocatalytic behaviour towards the HER was assessed by pseudo-steady-state polarization curves, electrochemical impendance spectroscopy (EIS) and hydrogen discharge curves in alkaline media.

II. Experiments

A. Preparation of Electrodes

The supporting macroporous Ni electrodes have been obtained by means of the electrodeposition at high current densities as it is described in [20].

For the synthesis of Au nanoparticles, a $2.5 \cdot 10^{-4}$ M tetrachloroauric acid solution was prepared and heated to 100ºC. 25 mL of a 0.5 wt.% sodium citrate were added at the hot solution. The citrate ions are responsible for the reduction of Au (III) ions to Au (0) and also for being complexing agents of the formed nanoparticles. Thus, the nanoparticle colloidal suspension is stabilized.

Macroporous Ni electrodes were coated with gold slurry by dip coating. Prior to the coating, the gold suspension was modified to increase viscosity and lower surface tension by addition of Hidroxi Etil Cellulose (0.5 wt.%) and BYK 347 (1 wt.%). Three Ni electrodes were coated: the first was dip coated twice allowing it to dry between the two immersions. The second electrode was dipped four times and the third six times. All electrodes were treated thermally in a tubular furnace at 350 ºC for 1 hour employing a nitrogen atmosphere.

The particle size distribution of gold suspension was analyzed by Dinamic Light Scattering (Zetasizer Nano S90, UK). A ZEISS ULTRA 55 field emission scanning electron

V. Pérez-Herranz, C. González-Buch, and E. M. Ortega are with Ingeniería Electroquímica y Corrosión (IEC), Departamento de Ingeniería Química y Nuclear, Universitat Politècnica de València, Camino de Vera s/n, 46022 Valencia, Spain (phone: +34-96-387-76-32; fax: +34-96-387-76-39; e-mail: vperez@iqn.upv.es).
S. Mestre. Instituto de Tecnología Cerámica, Campus Universitario Riu Sec, Av.Vicent Sos Baynat s/n,12006. Castellón, Spain.

microscope (FE-SEM) coupled with an Energy-Dispersive X-Ray (EDX) analysis was used to observe and confirm the presence of the Au nanoparticles on the macroporous Ni support.

B. Electrochemical Measurements

The developed electrodes were characterized by means of polarization curves, electrochemical impedance spectroscopy and hydrogen discharge curves in oxygen free 30 wt.% KOH solutions.

Polarization curves were potentio-dynamically recorded from -1.60 V vs Ag/AgCl up to the equilibrium potential, at a scan rate of 1 mV s^{-1}, and at six different temperatures: 30, 40, 50, 60, 70 and 80ºC. Before the tests, the working electrode was held at -1.60 V vs Ag/AgCl in the same solution, in order to reduce the oxide film existing on the porous surface electrode layer, for the time needed to establish reproducible polarization diagrams.

EIS measurements were performed after obtaining the polarization curves at different cathodic over-potentials, and at the following temperatures: 30, 50, and 80ºC. The measurements were made in the frequency range of 10 kHz to 3 MHz. Ten frequencies per decade were scanned using a sinusoidal signal of 10 mV peak-to-peak. The complex nonlinear least square (CNLS) fitting of the impedance data was carried out with the ZView 3.0 software package.

In order to obtain the hydrogen discharge curves, a progressively increasing voltage was applied, starting from 0 V between the anode (smooth Ni) and cathode (working electrode) and going up to 3 V. With the aid of these curves, the minimum discharge potentials were determined experimentally for each electrode pair.

The electrochemical measurements were carried out in an electrochemical cell developed by the Dpto. Ingeniería Química y Nuclear of the Polytechnic University of Valencia [21]. This cell allows monitoring the volume of gas generated at the anode and the cathode and to control the temperature (see Fig. 1).

III. Results

A. Morphologic Characterization of the Electrodes

Fig. 2 shows the particle size distribution, it can be seen the particle size presents a monomodal distribution, with a very sharp band between 10 and 50 nm. The characteristic parameters d10, d50 and d90 were 14, 20 and 31 nm respectively. The gold suspension was analyzed by SEM (Fig. 3). It was observed a homogeneous distribution of spherical particles.

Fig. 4 shows the FE-SEM images at different magnifications. In Fig. 4 (a) it can be seen that the macrostructure is the typical which corresponds to the Ni electrodes obtained at high current densities [20], [22]. In Fig. 4 (b), with higher magnifications, the Au nanoparticles can be observed onto the electrode surface as white points. The EDX analysis has confirmed the presence of Au and the at. % onto the electrode surface were 2.29, 0.88 and 0.51 at 2, 4 and 6 immersions respectively. As it can be seen, the at. % of Au onto the electrode surface decrease as the number of immersions increase. Moreover, increasing the number of immersions produce some damages on the electrode surface as it can be observed in Figs. 5 (a) and (b). In the electrode with only two immersions, the electrode surface is practically identical before and after the immersions and no damages can be detected.

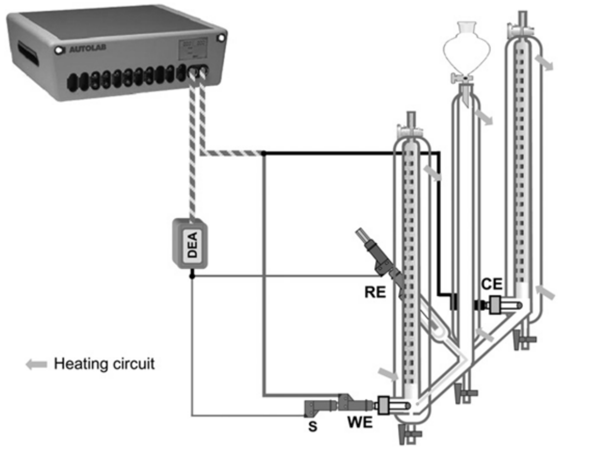

Fig. 1 Electrochemical cell (P200803389) and electrical connections

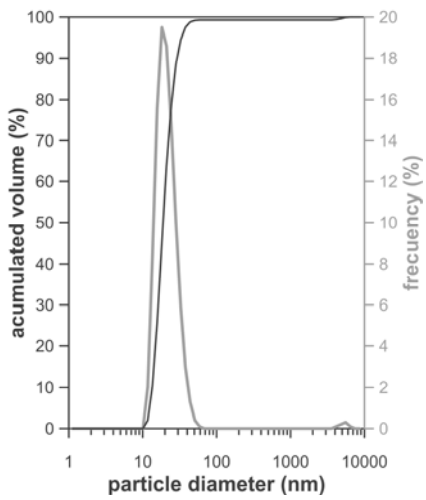

Fig. 2 Particle size distribution of gold nanoparticles suspension

B. Polarization Measurements

The electrocatalytic behaviour towards the hydrogen evolution reaction (HER) of the developed macroporous Ni electrodes modified with Au nanoparticles has been studied by means of the pseudo-steady-state polarization curves and electrochemical impedance spectroscopy (EIS). These techniques allow obtaining the most relevant kinetic parameters and the real electrochemically active surface area and then to conclude about the intrinsic catalytic activity of the developed electrodes.

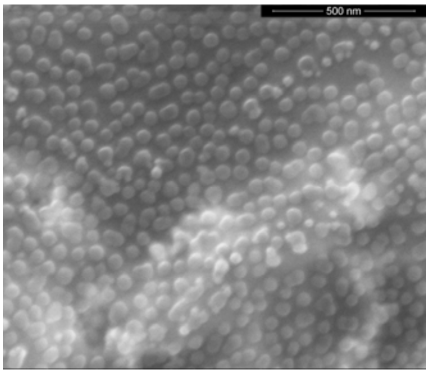

Fig. 3 SEM image of the gold nanoparticles suspension

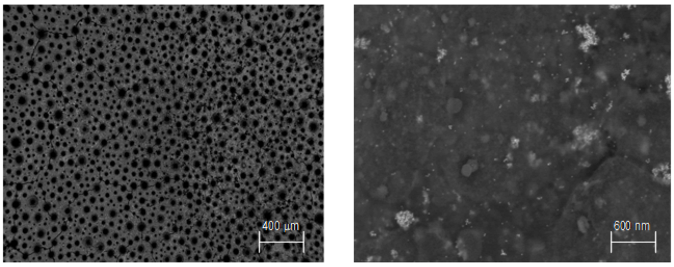

(a) (b)

Fig. 4 FE-SEM images of Macroporous Ni-Au NPS electrode at different magnifications

(a) (b)

Fig. 5 3D confocal laser micrographs before (a) and after (b) the six immersions

Fig. 6 shows the polarization curves recorded on KOH 30 wt.% at different temperatures between 30 and 80 ºC, showed a classical Tafelian behaviour, indicating that the HER on these electrodes is purely kinetically controlled reaction and it can be described by using the Tafel equation [20], [22]: $\eta = a + b \log j$, where η (V) represents the overpotential responsible of the current density j (A cm^{-2}), b (V decade^{-1}) is the Tafel slope, and a (V) is the intercept, related to the exchange current density j_0 (A cm^{-2}) by the equation: $a = (2.3RT)/(\alpha n_e F) \times \log j_0$. In turn, the charge transfer coefficient, α, can be obtained from the Tafel slope by using the relation: $b = -(2.3RT)/(\alpha n_e F)$, where n_e represents the exchanged electrons, R is the gas constant and F, the Faraday constant. By fitting the linear part of the Tafel curves recorded on the developed electrodes these kinetic parameters were obtained. Also, another important parameter that it was obtained to evaluate the catalytic activity of the electrodes was the over-potential at a fixed current density of -100 mA cm^{-2}, η_{100}. For an electrode, the lower the over-potential at a fixed current density, the lower the amount of energy required to produce a given amount of hydrogen, that is, the higher the catalytic activity of the electrode.

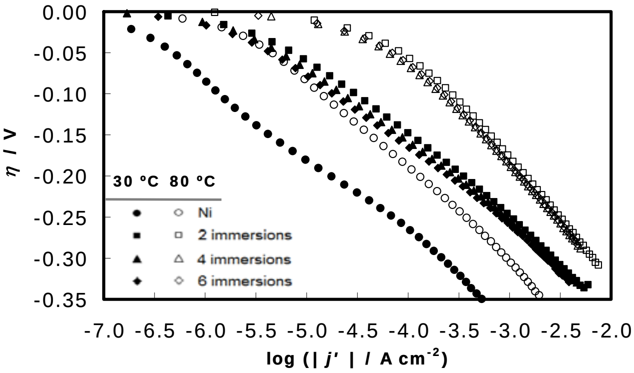

Fig. 6 Linear Tafel polarization curves recorded on 30 wt.% KOH solution at 30 ºC and 80 ºC, corrected with the surface roughness factor, r_f

The kinetic parameters calculated from the polarization curves are shown in Table I. The Tafel slope values ranging between 96 and 146mV dec^{-1}, close to the theoretical 120 mV dec^{-1} and the charge transfer coefficient is around to 0.5 indicating that the HER on these electrodes takes place by means of the Volmer-Heyrovsky mechanism [23], [24]. The exchange current density values are higher for the Au nanoparticles modified electrodes, likewise, this parameter increases with the number of immersions. Similarly, the η_{100} values are lower for electrodes with nanoparticles, showing its better catalytic activity. Again, the electrode with the highest number of infiltrations shows the lowest η_{100} and hence, higher overall catalytic activity. However, the catalytic activity evaluated with the parameters described above is related to the geometric electrode area and not to the real electrochemical area; therefore, it cannot conclude on the intrinsic catalytic activity of the developed electrodes. Electrochemical Impedance Study (EIS) permits to assess the real electrochemically active surface of the developed electrodes by giving the roughness factor, r_f, as the ratio between the double layer capacitance of a rough electrode and the double layer capacitance of a smooth electrode, which is 20 μF cm^{-2}.

Fig. 7 shows the Nyquist representation of the impedance response on the macroporous Ni and Macroporous Ni-Au NPs. This response is characterized by two semicircles, that is, the system consists of two time constants. The diameter of the semicircle obtained at high frequency is practically constant with the overpotential while the diameter of the semicircle obtained at lower frequencies diminishes as the overpotential applied increases. This is due to the fact that the adsorption process is facilitated and the charge-transfer process dominates the impedance response as the potential increases. Hence, having into account the values of α and the Tafel slopes determined from the polarization curves, and the information extracted from the EIS experiments, it can be concluded that the HER is controlled by the Volmer-Heyrovsky step [23], [24].

TABLE I
KINETIC PARAMETERS OF THE HER AND ROUGHNESS FACTOR OBTAINED FROM THE POLARIZATION CURVES AND EIS RECORDED IN 30 WT.% KOH SOLUTION AT DIFFERENT TEMPERATURES

	Temperature (ºC)		
Catalyst	30	50	80
Ni			
b (mV dec^{-1})	96.2	114.3	127.5
i_0 (mA cm^{-2})	0.05	0.11	1.04
α	0.62	0.56	0.55
η_{100}	248.2	347.1	252.8
r_f	741.5	643.0	615.1
i_0' (μA cm^{-2})	0.06	0.16	1.72
2 immersions			
b (mV dec^{-1})	146.3	173.4	217.4
i_0 (mA cm^{-2})	1.51	4.40	19.74
α	0.41	0.37	0.32
η_{100}	264.5	228.8	150.5
r_f	392.6	428.9	336.8
i_0' (μA cm^{-2})	3.85	10.26	58.61
4 immersions			
b (mV dec^{-1})	137.7	158.9	202.7
i_0 (mA cm^{-2})	1.46	4.37	22.55
α	0.44	0.40	0.35
η_{100}	249.2	211.8	130.2
r_f	553.9	597.5	514.6
i_0' (μA cm^{-2})	2.22	7.14	39.4
6 immersions			
b (mV dec^{-1})	123.5	143.4	195.0
i_0 (mA cm^{-2})	1.10	7.12	25.72
α	0.49	0.45	0.36
η_{100}	241.4	201.2	115.5
r_f	644.1	694.8	569.9
i_0' (μA cm^{-2})	1.71	10.25	45.13

This impedance response was correctly modeled by the equivalent circuit of two time constants in series (2TS) proposed by [25], consisting of the solution resistance, RS, in series two parallel CPE-R elements. This circuit connects the high frequency CPE-R element with the electrode porosity and the low frequency CPE-R to the kinetics of the hydrogen evolution reaction. The double layer capacitance of a porous electrode is given by the expression of Brug: $C_{dl} = [Q_2 /((R_S + R_p)^{-1} + R_{ct}^{-1})^{(1-n_2)}]^{1/n_2}$, where Q_2 and n_2 are the parameters of the constant phase element at low frequencies; R_p is the resistance of the first CPE-R element related to the porosity and R_{ct} is the resistance of the second CPE-R, which is related to the charge transfer resistance.

The parameters of the equivalent circuit were obtained by the adjustment of complex non-linear least squares (CNLS) with the software Zview 3.0. The roughness factor values of the macroporous electrodes are included in Table I. As can be seen both macroporous electrodes have a roughness factor in the same order of magnitude and the slightly differences may be due to the difference of the bubbles formed during the electrodeposition process.

In order to evaluate the intrinsic catalytic activity of the electrode is necessary to obtain the kinetic parameters related to the electrochemically active area and not to the geometric area. Therefore the exchange current densities values corrected with the roughness factor, j_0' were obtained for the developed macroporous electrodes and are included on Table I. As can be seen from the data on the table, the nanoparticles modified electrode has higher intrinsic catalytic activity than both nickel electrodes which present similar intrinsic catalytic activity.

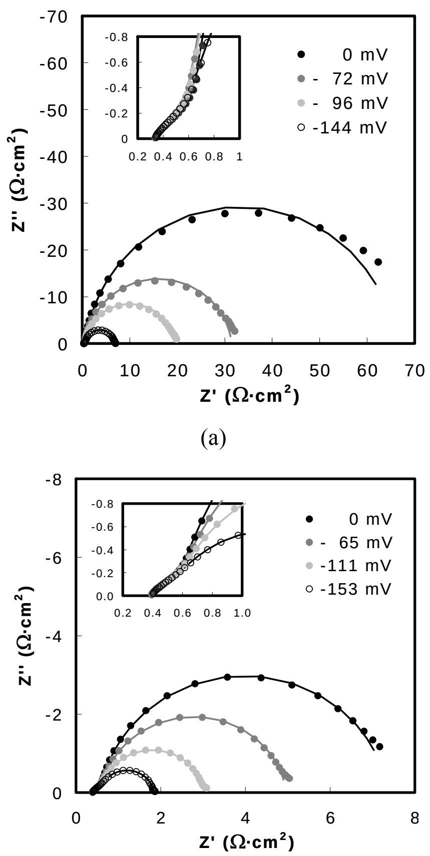

(a)

(b)

Fig. 7 Nyquist representation of the impedance data obtained in 30 wt.% KOH solution at 50ºC for Macroporous Ni electrode (a) and for Macroporous Ni-Au Nps (b)

C. Hydrogen Discharge Curves

In order to evaluate the suitability of the developed cathode for the most economical electrolysis process, current-cell potential curves (hydrogen discharge curves) have been obtained. All these tests were performed in the P200803389 cell [21]. It is a thermostated three-electrode cell that allows monitoring the volume of gas generated at the anode and the cathode. Fig. 8 shows the hydrogen discharge curves obtained using as cathodes both the Ni-Au and the Ni electrodes in 30 wt.% KOH solution at 30ºC. After the discharge of gasses, there is a rapid increase in the current with increasing applied voltage, because of the evolution of hydrogen at the cathode and oxygen at the anode. As seen in Fig. 8, the discharge of gasses starts at lower potential for the Ni-Au electrode, and the current passing through the solution is larger with this cathode, compared with the Ni cathode, at all potentials.

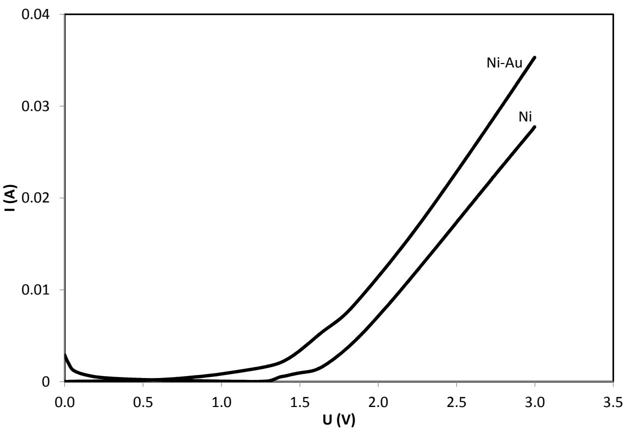

Fig. 8 Hydrogen discharge curves recorded on Ni-Au and Ni electrodes in 30% wt. KOH solution at 30ºC

IV. Conclusion

Ni macroporous electrode was synthesized by galvanic deposition at high current densities and then modified with Au nanoparticles to evaluate their electrocatalytic behaviour towards the hydrogen evolution reaction (HER) in alkaline media by means the pseudo-steady-state polarization curves and electrochemical impedance study (EIS). Main results of this research allowed us to enhance that:

Au nanoparticles have been successfully synthesised and characterized, manifesting a homogeneous distribution of spherical particles.

Macroporous Ni electrodes have the typical macrostructure which corresponds to the Ni electrodes obtained at high current densities and the incorporation of Au nanoparticles seems not to affect the macrostructure.

From Tafel polarization data it is clear that the Macroporous Ni-Au NPs electrocatalyst shows higher catalytic activity towards the HER than the smooth and macroporous Ni electrodes.

EIS permits to obtain the electrochemically active area by means of the roughness factor value, r_f, and to conclude about the intrinsic catalytic activity by means the exchange current densities values corrected to the r_f. From these values it is clear that the Au nanoparticles improve the intrinsic catalytic activity of the Ni electrodes.

Acknowledgment

The authors acknowledge the support of Generalitat Valenciana (PROMETEOII/2014/009).

References

[1] T. N. Veziroglu, F. Barbir, "Hydrogen - the wonder fuel," *Int. J. Hydrogen Energy*, vol. 17, pp. 391-404, 1992.

[2] W. B. Elosta, T. N. Veziroglu, "Solar hydrogen energy system for a Libyan coastal county," *Int. J. Hydrogen Energy*, vol. 15, pp. 33-44, 1990.

[3] W. Hug, J. Divisek, J. Mergel, W. Seeger, H. Steeb, "Highly efficient advanced alkaline electrolyzer for solar operation," *Int. J. Hydrogen Energy*, vol. 17, pp. 699-705, 1992.

[4] A. G. Garciaconde, F. Rosa, "Solar hydrogen-production - A Spanish experience," *Int. J. Hydrogen Energy,* vol. 18, pp. 995-1000, 1993.

[5] C. González-Buch, I. Herraiz-Cardona, E. Ortega, J. García-Antón, V. Pérez-Herranz, "Synthesis and characterization of macroporous Ni, Co and Ni–Co electrocatalytic deposits for hydrogen evolution reaction in alkaline media," *Int. J. Hydrogen Energy*, vol. 38, pp. 10157-10169, 2013.

[6] I. Herraiz-Cardona, C. González-Buch, C. Valero-Vidal, E. Ortega, V. Pérez-Herranz, "Co-modification of Ni-based type Raney electrodeposits for hydrogen evolution reaction in alkaline media," *J. Power Sources*, vol. 240, pp. 698-704, 2013.

[7] R. Solmaz, G. Kardaş, "Electrochemical deposition and characterization of NiFe coatings as electrocatalytic materials for alkaline water electrolysis," *Electrochim. Acta*, vol. 54, pp. 3726-3734, 2009.

[8] Y. Ullal, A.C. Hegde, "Electrodeposition and electro-catalytic study of nanocrystalline Ni-Fe alloy," *Int. J. Hydrogen Energy*, vol. 39, pp. 10485-10492, 2014.

[9] N.V. Krstajic, V.D. Jovic, L. Gajic-Krstajic, B.M. Jovic, A.L. Antozzi, G.N. Martelli, "Electrodeposition of Ni-Mo alloy coatings and their characterization as cathodes for hydrogen evolution in sodium hydroxide solution," *Int. J. Hydrogen Energy*, vol. 33, pp. 3676-36087, 2008.

[10] G.S. Tasic, S.P. Maslovara, D.L. Zugic, A.D. Maksic, M.P.M. Kaninski, "Characterization of the Ni-Mo catalyst formed in situ during hydrogen generation from alkaline water electrolysis," *Int. J. Hydrogen Energy*, vol. 36, pp. 11588-11595, 2001.

[11] M. Wang, Z. Wang, Z. Guo, Z. Li, "The enhanced electrocatalyitic activity and stability of NiW films electrodeposited under super gravity field for hydrogen evolution reaction," *Int. J. Hydrogen Energy*, vol. 36, pp. 3305-3312, 2011.

[12] M.A. Oliver-Tolentino, E.M. Arce-Estrada, C.A. Cortés-Escobedo, A.M. Bolarín-Miro, F. Sánchez-De Jesús, R. González-Huerta, A. Manzo-Robledo, "Electrochemical behavior of NixW1−x materials as catalyst for hydrogen evolution reaction in alkaline media," *J. Alloy Comp.* vol. 536, pp. S245-S249, 2012.

[13] R. Solmaz, A. Döner, G. Kardaş, "The stability of hydrogen evolution activity and corrosion behavior of NiCu coatings with long-term electrolysis in alkaline solution," *Int. J. Hydrogen Energy,* vol. 34, pp. 2089-2094, 2009.

[14] H. Dong, T. Lei, Y. He, N. Xu, B. Huang, C.T. Liu, "Electrochemical performance of porous Ni3Al electrodes for hydrogen evolution reaction," *Int. J. Hydrogen Energy*, vol. 36, pp. 12112-12120, 2011

[15] L. Wu, Y.H. He, T. Lei, B. Nan, N.P. Xu, J. Zou, B. Huang, C.T. Liu, "Characterization of porous Ni3Al electrode for hydrogen evolution in strong alkaline solution," *Mater. Chem. Phys*., vol. 141, pp. 553-561, 2013.

[16] G. Sheela, M. Pushpavanam, S. Pushpavanam, "Zinc–nickel alloy electrodeposits for water electrolysis," *Int. J. Hydrogen Energy*, vol. 27, pp. 627-633, 2002.

[17] M.A. Amin, S.A. Fadlallah, G.S. Alosaimi, "In situ aqueous synthesis of silver nanoparticles supported on titanium as active electrocatalyst for the hydrogen evolution reaction," *Int. J. Hydrogen Energy*, vol. 39, pp. 19519-19540, 2014.

[18] A. Kiani, S. Hatami, "Fabrication of platinum coated nanoporous gold film electrode: A nanostructured ultralow-platinum loading electrocatalyst for hydrogen evolution reaction," *Int. J. Hydrogen Energy*, vol. 35, pp. 5202-5209, 2010.

[19] R. Solmaz, "Electrochemical preparation and characterization of C/Ni-NiIr composite electrodes as novel cathode materials for alkaline water electrolysis," *Int. J. Hydrogen Energy*, vol. 38, pp. 2251-2256, 2013.

[20] I. Herraiz-Cardona, E. Ortega, L. Vázquez-Gómez, V. Pérez-Herranz, "Electrochemical characterization of a NiCo/Zn cathode for hydrogen generation," *Int. J. Hydrogen Energy*, vol. 36, pp. 11578-11587, 2011.

[21] J. García-Antón, E. Blaso-Tamarit, D. M. García-García, V. Guiñón-Pina, R. Leiva-García, V. Pérez-Herranz, P200803389, 2008.

[22] I. Herraiz-Cardona, E. Ortega, J. García Antón, V. Pérez-Herranz, "Assessment of the roughness factor effect and the intrinsic catalytic activity for hydrogen evolution reaction on Ni-based electrodeposits," *Int. J. Hydrogen Energy*, vol. 36, pp. 9428-9438, 2011.

[23] A. Lasia, A. Rami, "Kinetics of hydrogen evolution on Nickel electrodes," *J. Electroanal. Chem.*, vol. 294, pp. 123-141, 1990.
[24] O. Azizi, M. Jafarian, F. Gobal, H. Heli, M.G. Mahjani, "The investigation of the kinetics and mechanism of hydrogen evolution reaction on tin," *Int. J. Hydrogen Energy*, vol. 32, pp. 1755-1761, 2007.
[25] L.L. Chen, A. Lasia, "Study of the kinetics of hydrogen evolution reaction on Nickel-Zinc powder electrodes," *J. Electrochem. Soc.*, vol. 139, pp. 3214-3219, 1992.